Monthly velocity and seasonal variations of the Mont Blanc glaciers derived from Sentinel-2 between 2016-2024

Fabrizio Troilo[1,2], Niccolò Dematteis[3], Francesco Zucca[2], Martin Funk[4], Daniele Giordan[3].

[1]Fondazione Montagna sicura, Glaciers, snow and avalanche research area, Courmayeur, 11013, Italy.
[2] University of Pavia, Department of Earth and Environmental Sciences, Pavia, 27100, Italy.
[3]Research Institute for Geo-Hydrological Protection IRPI, Italian National Research Council, Turin, 10135, Italy.
[4] ETH-VAW, Versuchsanstalt für Wasserbau, Hydrologie und Glaziologie, Zurich, CH-8092, Switzerland.

Correspondence to: Niccolò Dematteis (niccolo.dematteis@irpi.cnr.it); Fabrizio Troilo (ftroilo@fondms.org).

Abstract. We investigated the temporal variability of the surface velocity of thirty glaciers in the Mont Blanc massif (European Alps). We calculated the monthly velocity between 2016 and 2024 using digital image correlation of Sentinel-2 optical imagery. The main objectives of the study are: (i) to characterise the variability of the velocity fields of such glaciers, referring both to their temporal (seasonal and interannual) and spatial variations; (ii) to investigate relationships between the morphology of glaciers and their kinematics. We measured monthly velocities varying from 12.7 m yr^{-1} to 487.4 m yr^{-1}. We observed an overall decrease in the velocity between 2016 and 2019 and an unexpected rise in 2020-2022, especially visible in most glaciers on the southern side of the massif. Considering the whole period, half of the glaciers showed positive acceleration, which reached values >4 m yr^{-2} in three glaciers. In general, the trend absolute value in the cold season is higher in case of positive acceleration and lower in case of negative acceleration. We found that smaller glaciers have a more pronounced seasonality, with winter-summer velocity differences of 50-100%. Finally, in 2016, 2018 and 2022, we observed an exceptionally high winter-summer velocity difference in the 0.3 km^2-wide Charpoua Glacier, when summer velocities increased by one order of magnitude.

1 Introduction

Glacier flow was one of the early drivers of glaciological interest and research since it was first studied. Its understanding and modelling evolved via the observations and findings of Somigliana (1938) in the early 1900s, Glen's laboratory experiments (Glen, 1952), followed by the interpretations of Nye (Nye, 1952) during the 1950s, to cite just a few, and have explained that the two main mechanisms of glacier flow rely on ice deformation and basal sliding. However, the motion of Alpine glaciers is largely related to basal sliding (Willis, 1995). Because continuous monitoring of sliding velocities in the field is extremely difficult and rarely achieved (Vincent and Moreau, 2016), measuring surface flow velocities can be a strong alternative approach. Nonetheless, the continuous monitoring of surface velocities of Alpine glaciers is complex on specific study sites, and very rarely has it been performed on a spatially distributed scale.

The flow of glaciers generally depends on a variety of physical parameters. The main physical parameter influencing ice velocity is the ice thickness (Jiskoot, 2011), which is indirectly related to the glacier trend in mass balance as it determines an evolution towards an increase or decrease in glacier thickness. Other parameters that influence ice flow are glacier surface slope, ice properties (temperature, density), bedrock conditions (hard, soft, frozen or thawed ice-bed contact), topography, the glacier's terminal area type (land, sea, ice shelf), but also air temperature and precipitation and their seasonality that influences subglacial hydrology (Jiskoot, 2011; Humbert et al., 2005; Cuffey and Paterson, 2010; Benn and Evans, 2014; Bindschadler, 1983).

The analysis of glacier surface velocity has a wide array of applications: it is a powerful climate change indicator (Beniston et al., 2018) and also an important input data for ice thickness models (Millan et al., 2022; Samsonov et al., 2021) and mass balance models that can also approximate sea-level rise contribution by glaciers (Zekollari et al., 2019). In the field of glacial hazards, it is used as an indicator for the detection of glacier surges with space-borne measurements (Kamb, 1987; Kääb et al., 2021), and accelerations that can result in glacier-related hazards using ground-based sensors (Pralong and Funk, 2006; Giordan et al., 2020). Measurements of the surface velocity of glaciers can be achieved by terrestrial techniques (Dematteis et al., 2021) such as topographic measurements of stakes or fixed points on the glacier (Stocker-Waldhuber et al., 2019), GNSS repeated or continuous surveys (Einarsson et al., 2016), digital image correlation of oblique photographs (Evans, 2000; Ahn and Box, 2010) and terrestrial radar interferometry (Luzi et al., 2007; Allstadt et al., 2015). Considering remote sensing solutions, glacier surface velocities can be measured by different aerial and space-borne sensors. In recent decades, public access to satellite optical and radar data (especially from Sentinel and Landsat constellation satellites), as well as the commercial availability of very high resolution (30 cm to 3 m ground resolution) optical imagery (Deilami and Hashim, 2011) and radar data (Rankl et al., 2014), have given great input to glaciological research. In particular, Sentinel-2 optical imagery is widely used in glaciological studies and has been tested in the literature on various environments (Paul et al., 2016; Millan et al., 2019). Nowadays, the automated processing of ice velocity maps with global coverage from satellite imagery is freely available online from web-based platforms such as the GoLIVE datasets (Fahnestock et al., 2016), the ITS_LIVE data portal (https://its-live.jpl.nasa.gov/) or the FAU-Glacier portal (RETREAT, 2021 Ice surface velocities derived from Sentinel-1, Version 1; http://retreat.geographie.uni-erlangen.de/search). The availability of such datasets is very relevant globally. Still, their application to Alpine glaciers is limited due to their relatively coarse spatial resolution - e.g., 300x300 m (GoLIVE), 120x120 m (ITS_LIVE) - which can provide data on just a few of the largest Alpine glaciers. Moreover, for the ITS_LIVE dataset, the velocity maps are calculated at a resolution of 240 m and statistically downscaled to 120 m, which has major limitations for small mountain glaciers. The adopted resolution is a trade-off between computational effort and the best resolution of the output that must cope with the global availability of the analysis. Limiting the processing of images at a regional scale decreases the computational effort compared to global products and makes it easier to obtain higher resolution velocity maps that allow Alpine glaciers to be investigated (Berthier et al., 2005), even though very small glaciers (i.e., width <250 m) are still difficult to analyse (Millan et al., 2019).

Recent studies using different techniques have measured spatio-temporal variations of ice velocity on large valley glaciers in an Alpine environment, like the Argentière (Vincent and Moreau, 2016) and Miage glaciers (Fyffe, 2012) as well as on steep glacier snouts (e.g., Planpincieux Glacier (Giordan et al., 2020)) but a spatially distributed analysis at a regional scale of the variations of velocities over glaciers with different morphological characteristics is, as of today, still lacking in the Alpine environment. Millan et al. (2022) calculated the velocities of world glaciers, but they considered a specific analysis period (2017-2018) not considering velocity variations in time, while Rabatel et al. (2023a) performed a comparison between yearly aggregated velocity maps between 2015 and 2021 over three different alpine massifs.

Other studies focused on long-term glacier velocity records in the Mont Blanc Massif: at the Argentière Glacier (Vincent and Moreau, 2016) and Miage Glacier (Smiraglia et al., 2000; Fyffe, 2012). At Argentière Glacier, a unique series of continuous basal sliding measurements existed from 1997 and was still active as of 2022 (Vincent et al., 2022; Nanni et al., 2020). The whole series indicates a general decrease in basal sliding velocities (Vincent and Moreau, 2016) since the end of the 1990s. This general decrease has shown a strong correlation with the negative mass balance of the glacier, which agrees with the conceptual model from Span and Kuhn (2003), in which the glacier flow variation is primarily driven by the mass balance of the accumulation area in the previous year (as it determines glacier thickness variations). Seasonal field surveys conducted at Argentière Glacier from the 1950s document a longer data series than the basal sliding measurements start in 1997, and an increase in surface velocities was measured during a period of positive mass balances in the early 1980s (Vincent

and Moreau, 2016). The same trend was highlighted by Span and Kuhn (2003) for at least six other glaciers: Saint Sorlin in France, Gietro and Corbassiere in Switzerland; Pasterze, Vernagtferner and Odenwinkelkees in Austria. At Miage Glacier, surface velocities have been measured historically by different authors (Diolaiuti et al., 2005; Smiraglia et al., 2000; Fyffe, 2012; Lesca, 1974; Pelfini et al., 2007; Deline, 2002) and also show a general velocity decrease in recent decades (Smiraglia et al., 2000; Fyffe, 2012). Glaciers such as Miage and Argentière, reach a low altitude and have flat and little crevassed valley tongues, for this reason, they have often been historically chosen for glaciological field surveys (Span and Kuhn, 2003). Therefore, the knowledge of Alpine glacier kinematics is generally mostly related to this type of glacier, which can be significantly different compared to the other glaciers analysed in this study.

Globally, glacier slowdown linked to a negative mass balance trend was also shown for six different regions around the globe and dates spanning from 1953 to 2009 by Heid and Kääb (2012b) by an analysis of remotely-sensed optical images. Specific analysis of velocity trends and glacier mass loss showed generalized decreasing velocity trends over different regions of High Mountain Asia between 2000 and 2017 and a strong correlation with the negative mass balance trend (Dehecq et al., 2019).

The main purposes of this study are the production of eight-year-long velocity time series of the surface velocity of thirty glaciers at a massif scale, derived from Sentinel-2 optical images, as well as an integrated analysis of morphological and kinematic features of such glaciers. The identification of possible trends in the velocity time series is a major objective of the present study. We observed different behaviours of surface velocity and identified a relationship between seasonality and glacier size.

2 Area of study

The study area is the Mont Blanc massif. It is located in the western part of the European Alps bordering France, Italy and Switzerland (Fig. 1) and culminates at 4809 m a.s.l. with the Mont Blanc summit, the highest peak in Central Europe. Many other peaks in the Mont Blanc massif reach well above 4000 m a.s.l. and the entire area is highly frequented with famous tourist resorts such as Courmayeur and Chamonix attracting thousands of tourists every year.

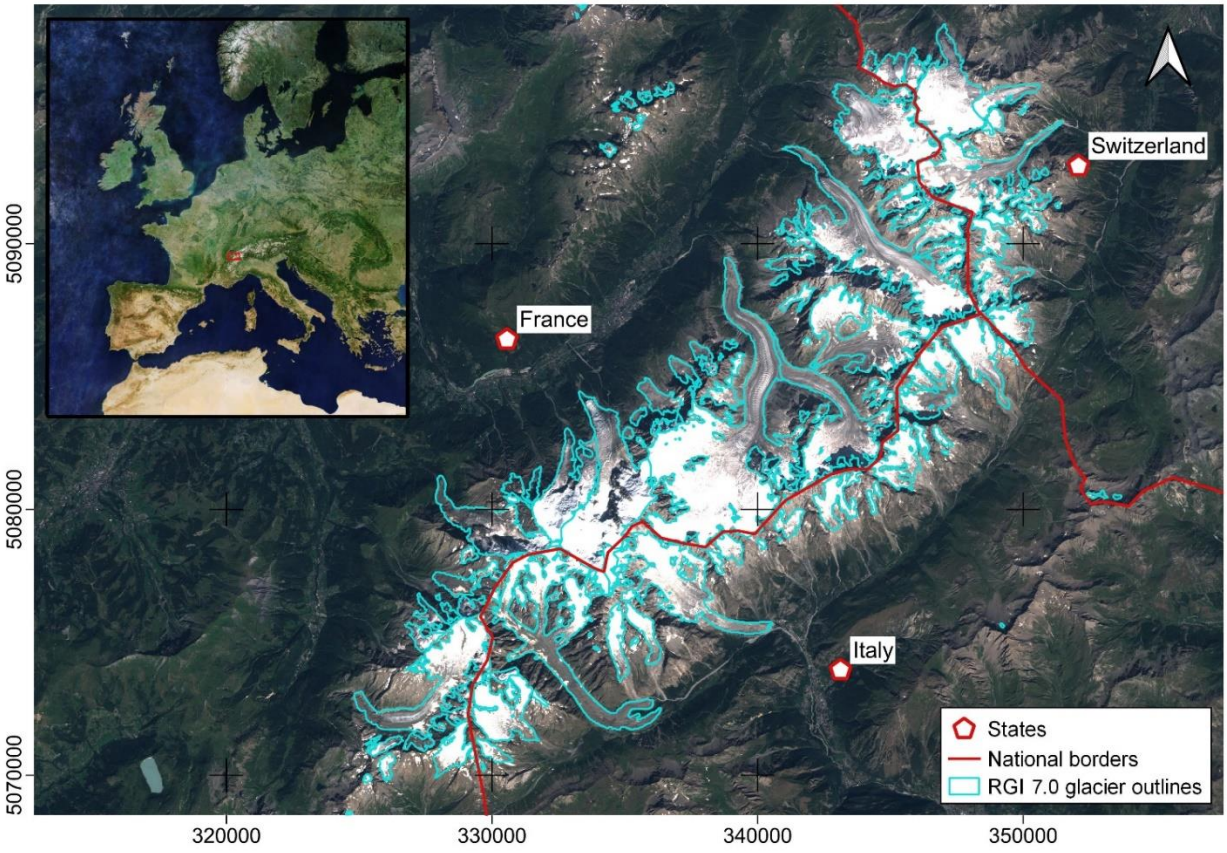

Fig. 1 Study area of the Mont Blanc massif. Background: true colour image (cloud-free Europe mosaic in the upper left panel), courtesy of the Copernicus Open Access Hub (https://scihub.copernicus.eu, last access: 10 September 2023).

The total surface of glaciers in the Mont Blanc massif is equal to 169 km^2 and totals 116 glaciers, according to the Randolph glacier inventory (RGI 7.0) (RGI Consortium, 2023). The inventory refers to 2003 (Pfeffer et al., 2014; Arendt et al., 2017). Forty glaciers are very small, covering an area of less than 0.1 km^2, forty-seven have surfaces between 0.1 and 1 km^2, sixteen glaciers fall between 1 km^2 and 3 km^2, and thirteen glaciers have surface areas of more than 4 km^2.

The geological setting and the geomorphology of the Mont Blanc massif form a high mountain range with its main ridge line oriented in a southwest/northeast direction along the French-Italian border. The valley floors flanking the massif have low altitudes - in the range of 1000-1500 m a.s.l. - resulting in steep slopes originating from the highest peaks with large vertical altitudinal differences. The meteo-climatic local conditions on the massif are of a continental type, but orographic effects on the predominant incoming weather fronts produce larger precipitation compared to nearby regions (Gottardi et al., 2012).

The Argentière Glacier is the only glacier with regular mass balance measurements in the World Glacier Monitoring Service (WGMS) 'Reference Glaciers' dataset in the Mont Blanc Massif (Zemp et al., 2009). The Argentière Glacier has shown a general negative mass balance trend since the early 1990s (Vincent, 2009), in line with mass balances of other Alpine glaciers and glaciers from other mountain ranges across the globe. Geodetic mass balance measurements of the Thoula Glacier, a small glacier on the border between France and Italy at altitudes between 2900 and 3300 m a.s.l., represent well the local

meteo-climatic conditions that result in slightly less negative mass balance trends compared to other glaciers in the Alps (Zemp et al., 2021; Zemp et al., 2020; Mondardini et al., 2021).

A more spatially distributed analysis of mass balances in the Mont Blanc region has also been outlined in the literature employing geodetic mass balances of the whole Mont Blanc massif using stereo satellite imagery from the Pléiades and Spot satellite constellations (Berthier et al., 2014; Beraud et al., 2023). The trend outlined by Berthier et al. (2023) at the massif scale reflects data trends comparable to the glaciological mass balances of WGMG reference glaciers in the Alps. Glaciers at lower altitudes show larger ice volume losses and subsequent substantial glacier front retreats (Paul et al., 2020), while glaciers at higher altitudes suffer less acute volume loss and shrinkage. Large differences in the glacier frontal position, especially for the lower altitude terminating glaciers, can be well assessed by the difference of the terminus position in recent satellite imagery compared to the position outlined on the RGI 7.0.

3 Materials and Methods

3.1 General workflow

In this paper, we analysed the Copernicus - ESA Sentinel-2 optical satellite imagery dataset available for the study area. In addition, we used Pleiades Stereo derived digital elevation models (DEMs) to retrieve morphometric data of glaciers and publicly available modelled ice thickness data from Millan et al. (Millan et al., 2022). We used digital image correlation (also known as feature tracking) to produce monthly-averaged and multi-year averaged velocity maps to investigate variations of glacier surface velocity in time and space over the selected glaciers. We can hereby summarize the workflow that was used (Fig. 2).

The input data are a DEM of the study area, the RGI glacier outlines, the modelled glacier thickness and the stack of Sentinel-2 images in the reference period. The input DEM is used to obtain morphometric data of the glacier, while the RGI glacier outlines and the selected satellite imagery is used to choose suitable glaciers for surface glacier velocity analysis. After the glacier selection, we updated the RGI glacier outlines according to the current glacier extensions. Selected imagery is processed with digital image correlation to obtain glacier velocities. The glacier flowlines of the RGI are then used, together with the updated glacier outlines and the mapped equilibrium line altitudes (ELAs), to identify sampling areas to extract velocity time series. ELAs are manually digitized each year by the analysis of Sentinel-2 imagery. Subsequently, the time series are analysed to identify general trends, seasonal patterns or particular kinematic behaviours. Finally, the velocity dataset is analysed in relation to the morphological characteristics (in particular their size) of the glacier.

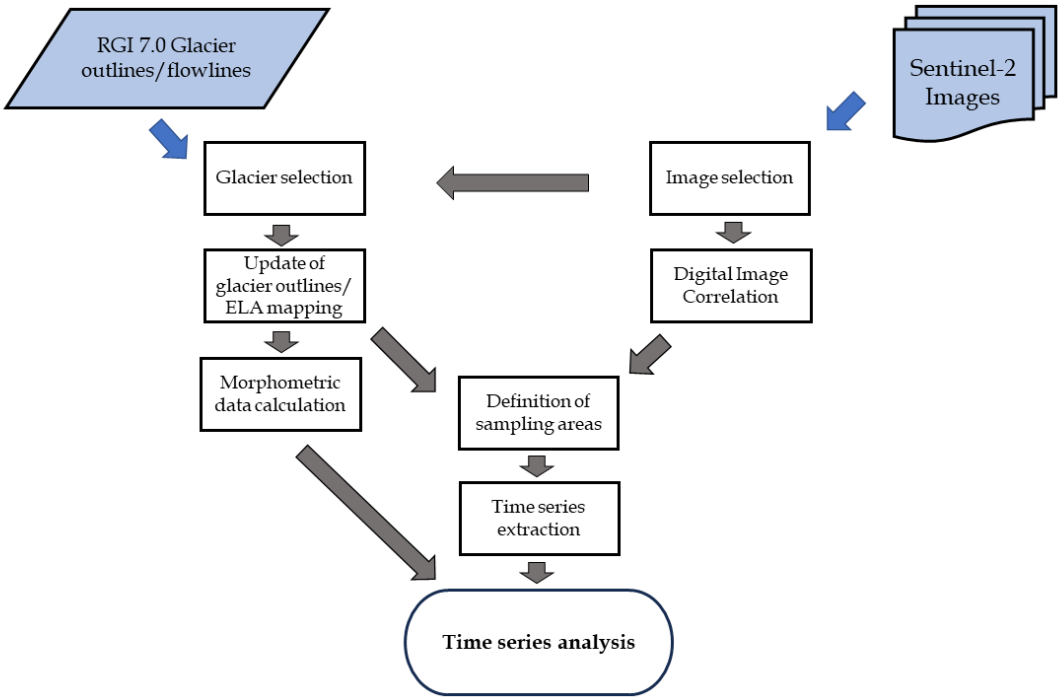

Fig. 2 Workflow of the present study. The input datasets are evidenced in light blue while the processing steps are indicated in white boxes.

3.2 Sentinel-2 optical satellite imagery

We adopted Sentinel-2 optical images acquired between February 2016 and February 2024. We chose to start the analysis in 2016 because it was the first full year of acquisition by the satellite. Based on different publications (Kääb et al., 2016; Millan et al., 2019), the geometric misregistration of Sentinel-2 can show up to 1.5 pixel offsets in the horizontal plane even if it can be usually closer to a value of 0.5 pixels, which corresponds to the absolute geolocation specification by ESA. Therefore, an image co-registration process or a correction of stable ground shifts is normally needed for multitemporal analyses.

To select the images, we defined the presented approach: (i) to maximize the geometric and geo-referencing precision, we adopted images acquired from the same orbit and tile (GRANULE T32TLR, relative orbit 108); (ii) to reduce the impact of clouds, we carried out a visual check of all images with a cloud cover percentage lower than 80% (as detected by the Copernicus cloud cover estimation algorithm) on the whole tile, which were 323 in total (150 from Sentinel 2B and 173 from Sentinel 2A). From this dataset, we extracted a subset of 123 cloud-free images on the selected glacier areas via the visual inspection of the individual images. We adopted this manual selection to maximize the quality of the images; in the case of the Mont Blanc massif (like in most mountainous areas worldwide), the local distribution of clouds can be extremely variable; in many cases, this can contribute to a considerable cloud percentage, even though high altitude areas may still be cloud-free.

The number of suitable images available per year varies from 10 to 20, with a yearly mean of 15 images in the following distribution: 2016: 10; 2017: 18; 2018: 11; 2019: 14; 2020: 13; 2021: 16; 2022: 20, 2023: 19, 2024: 2. The year 2016, and partially 2017, is influenced by the lack of Sentinel 2B images, which was launched on 7 March 2017.

To apply image correlation, we used the near-infrared band B08 at the processing level L1C, as suggested by previous studies (Kääb et al., 2016).

3.3 Glacier selection

To minimize the presence of noisy and unreliable velocity data, we performed a selection of glaciers from the RGI 7.0 dataset. In particular, we did not include in our study: A) glaciers with an area < 0.1 km^2, as those glaciers would be too small for the reliable extraction of velocity maps with 10 m resolution optical satellite imagery (Millan et al., 2019); B) glaciers showing strong variations of cast shadow; C) glaciers that lack surface features to be tracked (e.g., ice caps).

Selection of point B) was made by creating a stack of images acquired between October and March, when cast shadows appear on satellite imagery, especially on north-facing slopes. Subsequently, we manually identified glaciers that are subject to large variations of shadow on their surface. We used the scene classification map (SCL) class 11 (cast shadows), available in processing level L2A of the Sentinel-2 images. However, since shadows on glaciers may often be misclassified, we conducted a manual check to correct potential errors. Selection of point C) is made manually by selecting glaciers that show very even surfaces on Sentinel-2 images. This is normally noted in ice caps at higher altitudes or flat valley tongues.

The glacier selection process identified thirty glaciers with a total glacierised surface (in 2018) of 85.8 km^2. Compared to the total glacierised surface of the massif from RGI 7.0, this represents the covering of 50.8% of the total 169 km^2 and 25.9% in terms of number of glaciers; this rises to 39.5% if we consider the subset of seventy-six glaciers having a glacierised surface of more than 0.1 km^2. The selected glaciers are highlighted in Fig. 3 and listed in Table 1. Two of the selected glaciers are located in Switzerland, ten in France and eighteen in Italy. This distribution is mainly due to a small portion of the massif being located in Switzerland and the presence of more fragmented glacierised bodies on the Italian side. Seven of the thirty glaciers have been mapped as sub-areas compared to RGI 7.0 individual glacier bodies. A brief description of all the glaciers we analysed is found in section S1.1 to describe the location and geomorphological setting of the glaciers as well as highlight when a single glacier complex from the RGI 7.0 was divided into independent glacial bodies because of very distinct kinematic behaviour.

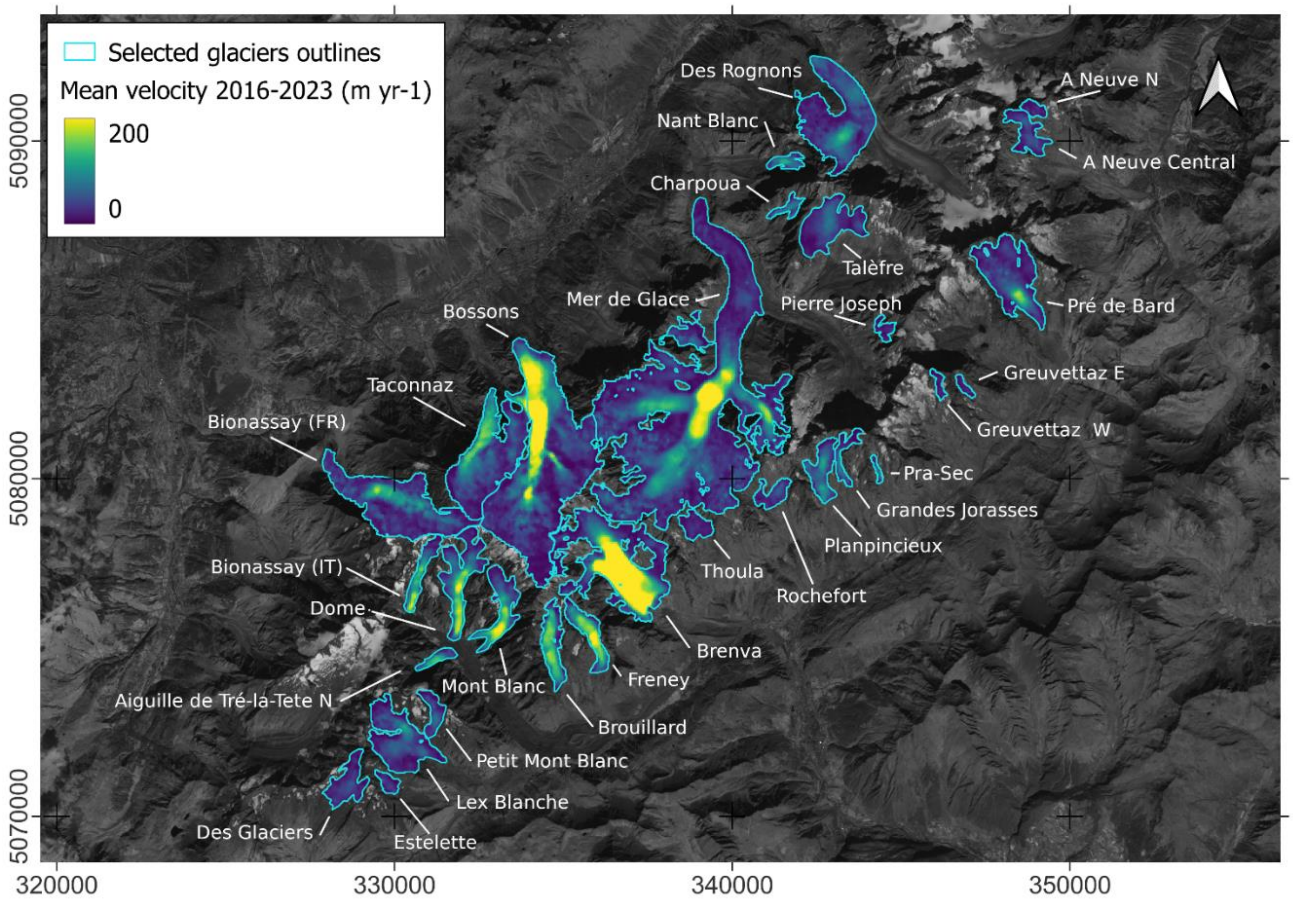

Fig. 3 Surface glacier velocity map averaged in the 2016-2024 period. Selected glaciers for specific analyses are outlined in cyan. Background: Sentinel-2 image (B08 band), courtesy of the Copernicus Open Access Hub (https://scihub.copernicus.eu, last access: 10 September 2023).

3.4 Glaciers' outline delineation and morphometric data calculation

Since the RGI 7.0 glacier outlines refer to 2003, we updated them to fit with the present glacier extensions and manually outlined them from Sentinel-2 imagery. We selected a cloud-free scene acquired on 28 August 2018 that represents well the conditions of the glaciers in the study period; True Color Image was used for this purpose. The main morphometric data that were determined for each glacier are summarized in Table 1. In some cases, a morphological indication that some parts of the glaciers could be considered independently from others and divided into individual kinematic domains was considered (Paul et al., 2022; Zemp et al., 2021). As the velocity maps confirmed distinct behaviours of some glacier parts, those glaciers were divided and mapped accordingly. The main examples are the tributary glaciers of the larger Miage Glacier complex, which all have distinct kinematic behaviour, well differentiated from the slow-moving, debris-covered main central valley tongue. Another example is the Talèfre Glacier, where, over the past twenty years, the western part of the glacier has become independent from the eastern portion.

The determination of morphometric data of sample glaciers was performed using altitudinal data from a 2 m resolution DEM obtained by processing Pleiades stereo pairs acquired in August 2018 (Berthier et al., 2014), while the mean glacier

thicknesses were extrapolated from globally modelled ice thickness data (Millan et al., 2022), which has an average uncertainty of 30%.

Table 1. Table with name and RGI identification codes of glaciers selected for analysis in the present study and main morphometric parameters. The elongation is the glacier length divided by its area.

Glacier name	RGI 7.0 ID	Area (km^2)	Length (m)	Min alt (m a.s.l.)	Max alt (m a.s.l.)	Avg slope (°)	Mean ice thickness (m)	Elongation (m^{-1})
A Neuve N	RGI2000-v7.0-G-11-00722	0.27	790	3084	3454	25.0	24	2.95
A Neuve Central	RGI2000-v7.0-G-11-00721	0.89	1800	2664	3554	26.3	26	2.02
Pre de Bard	RGI2000-v7.0-G-11-00716	3.01	3300	2360	3641	21.2	63	1.10
Greuvettaz E	RGI2000-v7.0-G-11-00708	0.20	990	2948	3582	32.8	12	5.03
Greuvettaz W	RGI2000-v7.0-G-11-00707	0.17	840	2704	3291	35.0	12	4.95
Planpincieux	RGI2000-v7.0-G-11-00703	1.01	2050	2627	3650	26.5	45	2.02
Grandes Jorasses	RGI2000-v7.0-G-11-00703	0.48	2110	2701	4206	35.5	15	4.38
Pra Sec	RGI2000-v7.0-G-11-00704	0.12	870	2536	3190	36.8	9	7.34
Rochefort	RGI2000-v7.0-G-11-00701	0.56	1000	2720	3301	30.3	25	1.78
Brenva	RGI2000-v7.0-G-11-00695	6.58	4490	2374	4766	28.0	80	0.68
Thoula	RGI2000-v7.0-G-11-00698	0.58	1080	2880	3416	26.5	25	1.85
Mont Blanc	RGI2000-v7.0-G-11-00688	0.76	2490	2776	3773	21.9	47	3.25
Dome	RGI2000-v7.0-G-11-00688	1.97	3550	2453	4121	25.1	51	1.80
Bionassay (IT)	RGI2000-v7.0-G-11-00688	1.35	2930	2467	3816	24.8	53	2.16

Aiguille Tre la Tete N	RGI2000-v7.0-G-11-00688	0.31	1360	2408	3010	24.0	78	4.34
Freney	RGI2000-v7.0-G-11-00693	1.02	2620	2420	3698	26.0	61	2.58
Brouillard	RGI2000-v7.0-G-11-00691	1.17	2730	2499	3972	28.3	52	2.34
Lex Blanche	RGI2000-v7.0-G-11-00674	2.64	2450	2467	3757	27.8	41	0.93
Petit Mont Blanc	RGI2000-v7.0-G-11-00674	0.56	1770	2863	3580	22.1	26	3.18
Estelette	RGI2000-v7.0-G-11-00673	0.29	950	2716	3214	27.7	24	3.26
Pierre Joseph	RGI2000-v7.0-G-11-00713	0.28	710	2920	3409	34.6	15	2.58
Nant Blanc	RGI2000-v7.0-G-11-00749	0.36	1150	2600	3351	33.1	33	3.17
Charpoua	RGI2000-v7.0-G-11-00751	0.32	1210	2650	3479	34.4	25	3.76
Des Glaciers	RGI2000-v7.0-G-11-00664	1.09	2050	2735	3815	27.8	31	1.88
Talèfre N	RGI2000-v7.0-G-11-00753	2.04	1950	2700	3550	23.6	39	0.96
Des Rognons	RGI2000-v7.0-G-11-00745	4.52	4290	2178	3800	20.7	102	0.95
Mer de Glace	RGI2000-v7.0-G-11-00757	23.56	12090	1774	4025	10.5	104	0.51
Bossons	RGI2000-v7.0-G-11-00773	11.32	6800	1691	4776	24.4	60	0.60
Taconnaz	RGI2000-v7.0-G-11-00774	4.99	4290	2043	4286	27.6	40	0.86
Bionassay (FR)	RGI2000-v7.0-G-11-00778	4.77	5240	1835	4287	25.1	40	1.10

3.5 Glaciers' surface velocity calculation

Digital image correlation is a common technique used to measure surface displacements using proximal (Evans, 2000; Ahn and Box, 2010; Schwalbe and Maas, 2017; Dematteis et al., 2024) and remotely sensed imagery (Scambos et al., 1992; Heid and Kääb, 2012; Marsy et al., 2021; Dematteis and Giordan, 2021). The processing chain performed in the present study uses the open-source Glacier Image Velocimetry (GIV) toolbox (Van Wyk De Vries and Wickert, 2021). GIV uses frequency-based correlation, can efficiently process large datasets and has been shown to perform well on glacier surface velocity measurements at different test sites (Van Wyk De Vries and Wickert, 2021). GIV calculates stable-ground shifts to correct for georeferencing errors; therefore, we created a stable ground mask composed of non-glacierized terrain surrounding the massif and fit a 2D second-degree polynomial to the residual velocities over stable ground in the x- and y- directions. To measure glacier surface velocities, we adopted the 'multi-pass' option, which updates displacement estimates over multiple iterations, refining initial coarse chip size displacement calculations using progressively smaller chip sizes. The initial chip size is automatically defined by GIV and cannot be smaller than 32x32 px. The overlap between matching windows was 0.5. Velocities higher than 1500 m yr^{-1} were considered unrealistic and discarded. The velocity map resolution was set to 40 m without resampling. Finally, we smoothed the velocity maps by applying a 3x3 median filter.

To produce the time series, given a specific image, we processed the first and second subsequent images (GIV order 2 time-oversampling). The minimum and maximum temporal repeat cycles were 10 and 120 days, respectively. We calculated 218 image pairs, with an average temporal baseline of 35 days (Sec. S8).

Subsequently, the velocities of image pairs were averaged on a monthly basis. We applied the weighted average included in GIV, where the weights are proportional to the fraction of time included in a given month over the total time gap between the image pairs. The presence of clouds or snow on the glacier surface made it impossible to extract reliable data in the following months: i) January 2017, ii) December 2020, January and February 2021 iii) September 2021. The gaps represent only five months on which we did not retrieve velocity data out of the eight years considered in the study (i.e., <5%). In Fig. 3, we present a velocity map with a resolution of 40 m. This was obtained by averaging all the single monthly velocity maps in the study period (2016-2024). In Fig. 4, we present an example of the obtained velocity map and the distribution of sampling areas over several chosen glaciers. All other parameters of the GIV processing were set at default parameters (Supplementary Materials section S5).

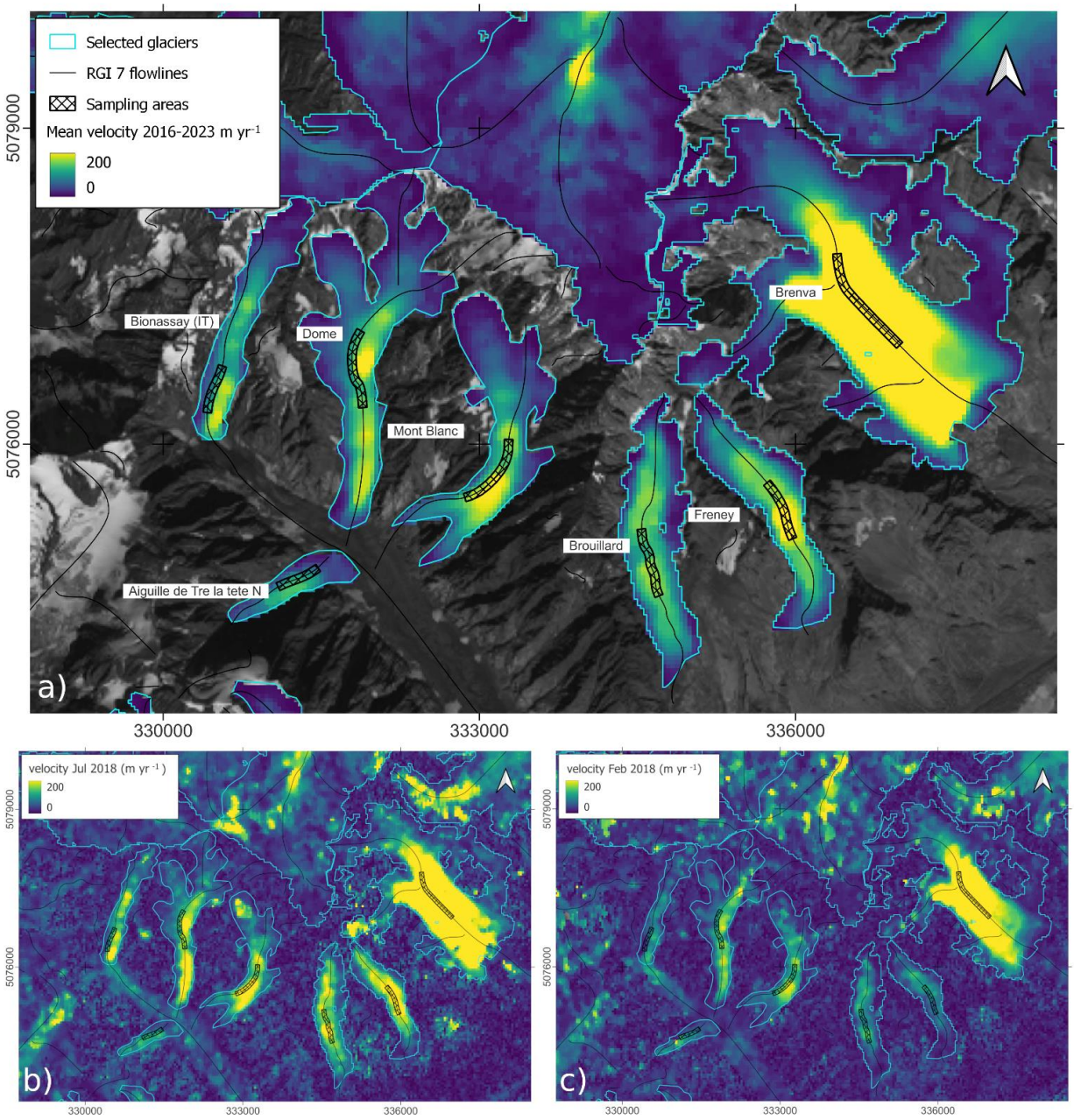

Fig. 4 a) Details of glacier surface velocity map averaged in the 2016-2024 period and sampling areas of selected sample glaciers. b, c) show monthly velocity maps of July and February 2018 respectively. Sentinel-2 imagery base map (B08 band), courtesy of the Copernicus Open Access Hub (https://scihub.copernicus.eu, last access: 10 September 2023).

3.6 Velocity time series analysis

Sampling areas were identified on the velocity maps to analyse the time series of the selected glaciers. Since the surface velocity of land-terminating glaciers is expected to be the highest in correspondence with the ELA (Nesje, 1992), we cropped the RGI 7.0 flowlines at the upper and lower altitudinal limits of the ELAs mapped between 2016 and 2023. Around this section of the ELA, we buffered an area of 40 m (Fig. 4). The velocity values included in the obtained polygons were averaged to produce the time series (i.e., the velocity was not calculated over the whole glaciers, but only in the region of the ELA).

Subsequently, we applied a quadratic locally weighted scatterplot smoothing (LOWESS) (Cappellari et al., 2013) evaluated on a rolling window of twelve months. Finally, we calculated the linear trend of the smoothed series using the Huber loss regressor (Huber, 1992). The Huber fit is robust against outliers; thus, sharp velocity fluctuations should not affect the obtained linear trends. To evaluate the statistical significance level of the fit, we consider the *t-statistics*, i.e., the ratio between the coefficient values and their standard errors. According to its definition, the t-statistics is expected to be low when the slope of the linear fit is low and/or when the slope is relatively low compared to the data variability.

We performed the principal component analysis (PCA) of the time series to investigate the overall behaviour of all the considered glaciers, and we weighted the time series according to the glacier area. The PCA is a multivariate analysis technique that allows a reduction in the dimensionality of a given dataset, increasing interpretability but minimising information loss. This is achieved by creating new, uncorrelated variables that successively maximise the variance of the dataset (Jolliffe and Cadima, 2016).

4 Results and discussion

4.1 Distributions of monthly velocities

Overall, considering the thirty glaciers we investigated in this study, the monthly velocity values range from 30-40 m yr^{-1}, typically reached during winter months by smaller glaciers, to > 400 m yr^{-1}, typically reached in summer/late summer by faster glaciers. The Brenva and the Bossons glaciers attain the highest velocities. In particular, monthly extreme values vary from 11.8 +/- 9.8 m yr^{-1}, reached on January 2022 by the Des Glaciers Glacier, to 487.4 +/- 10.8 m yr^{-1}, reached by the Brenva Glacier in July 2016. The mean surface velocities averaged over the period range from 29.9 +/- 10.9 m yr^{-1} at the Pierre-Joseph Glacier to 375.9 +/- 10.9 m yr^{-1} at the Brenva Glacier. The standard deviation of the velocity time series of single glaciers varies from 10.3 m yr^{-1} at the Pierre Joseph Glacier to 70.7 m yr^{-1} at the Charpoua Glacier. Fig. 5 presents the distributions of the raw monthly velocity of the considered glaciers.

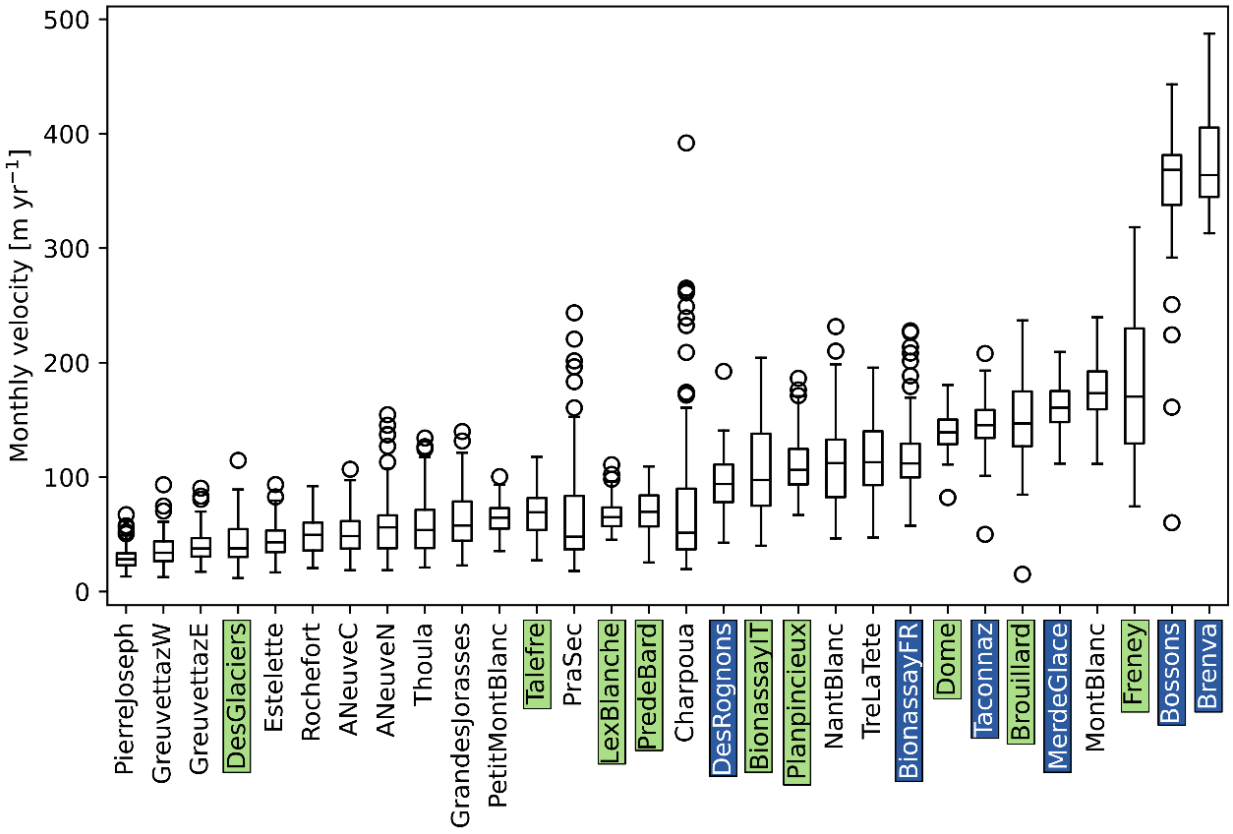

Fig. 5. Boxplot showing the glaciers' raw monthly velocity distributions. Glaciers are sorted by their median velocity. The background colours of the glacier names indicate their size: white < 1 km^2; green 1-4 km^2; blue >4 km^2. The boxes's limits and central line represent the first, second (i.e., the median) and third quartiles, respectively; the whiskers indicate the first/third quartiles minus/plus 1.5 IQR (interquartile range). The white circles are outliers.

4.2 Velocity time series

Large and thick glaciers generally have high velocities; two (Brenva and Bossons) show the highest values. The velocity values remain high throughout the year (Fig. 6). Brenva displays irregular seasonality variations, while Bossons has an almost absent seasonal cycle. Their morphology is complex - e.g., the slope varies considerably along their extent. In the present study, we concentrated the analyses on the middle sectors (near the ELA) of the glaciers, which are the fastest (Nesje, 1992). In the time series, the biggest glacier (Mer de Glace) appears slower because we extracted the monthly velocity over an area which does not entirely include the most active sector of the Mer de Glace Glacier (i.e., the Géant Ice Fall), where the velocity reached values >400 m yr^{-1}.

Medium-sized glaciers' morphology is less homogeneous, although most are generally gentler and thicker than average. We can divide the group into two sets based on the elongation ratio. Medium-sized glaciers, which are more elongated, generally feature strong kinematic activity, their velocity is higher than average with marked variability, and they often show a pronounced regular annual cycle, as in the cases of the Bionassay (IT), Brouillard, Mont Blanc and Freney glaciers. The second set of more "compact" glaciers shows lower mean velocities and has a minor amplitude of the seasonal variability. In particular, even though some display a regular seasonal cycle (e.g., Planpincieux, Dome, Rochefort), their velocity variability is much lower (Fig. 6).

Small glaciers show lower average velocities, but most show marked and regular seasonality. In this group, some very small glaciers (e.g., Greuvettaz W, Greuvettaz E, A Neuve N, Pierre Joseph) show a modest, irregular, or even non-detectable seasonal cycle since the velocity in winter is close to the measurement uncertainty (Fig. 6). It is worth highlighting that signals of potential velocity fluctuations could exist, but remotely sensed data are not currently suited for analysing such small glaciers.

On the other hand, Pra Sec and Charpoua, small steep elongated glaciers, feature very low minimum velocities (between 25 m yr^{-1} and 50 m yr^{-1}) and very marked peaks during which the velocity increased by one order of magnitude. These high velocity periods appear in summer/late summer, and extreme velocity changes from winter to summer velocities can be noticed. In 2016, 2018 and 2022, the summer velocity of Charpoua Glacier was exceptionally high compared to the usual. Moreover, in these years, the spatial distribution of velocities varied. The highest velocities were registered towards the frontal part of the glacier. At the same time, normally it was higher in the upper sector (Fig. 7). Pra Sec Glacier displays more regular annual speedups in the period analysed, every summer it had a clear velocity peak (except in 2018), particularly pronounced in 2016, 2020 and 2022. In both glaciers, possible glacier advances are prevented by the steep bedrock cliff at the snout, which causes the disintegration of the glacier by repeated ice falls from the terminus (Giordan et al., 2020; Pralong and Funk, 2006).

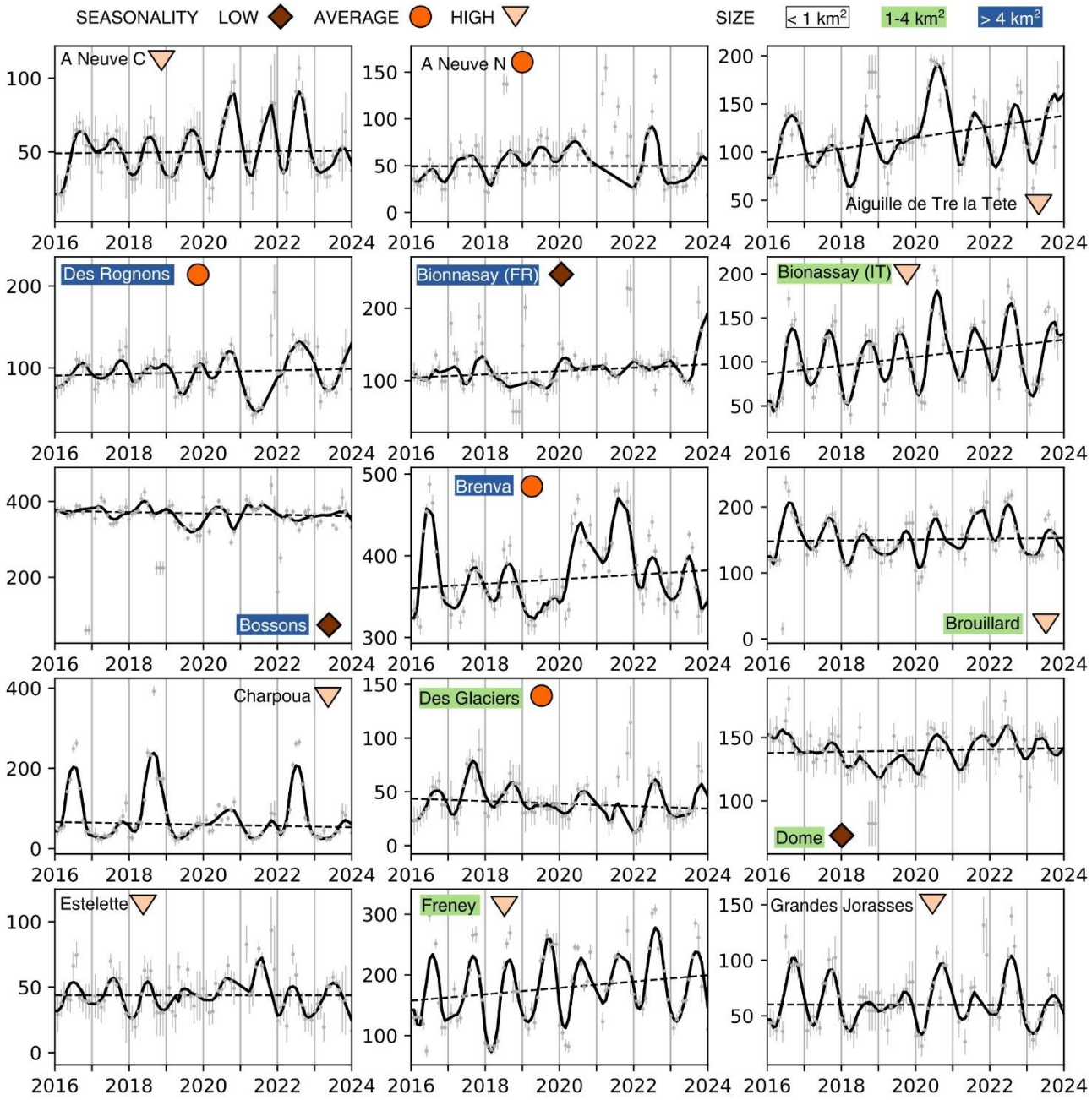
SEASONALITY LOW AVERAGE HIGH
SIZE < 1 km² 1-4 km² > 4 km²
A Neuve C
A Neuve N
Aiguille de Tre la Tete
Des Rognons
Bionnasay (FR)
Bionassay (IT)
Bossons
Brenva
Brouillard
Charpoua
Des Glaciers
Dome
Estelette
Freney
Grandes Jorasses

306

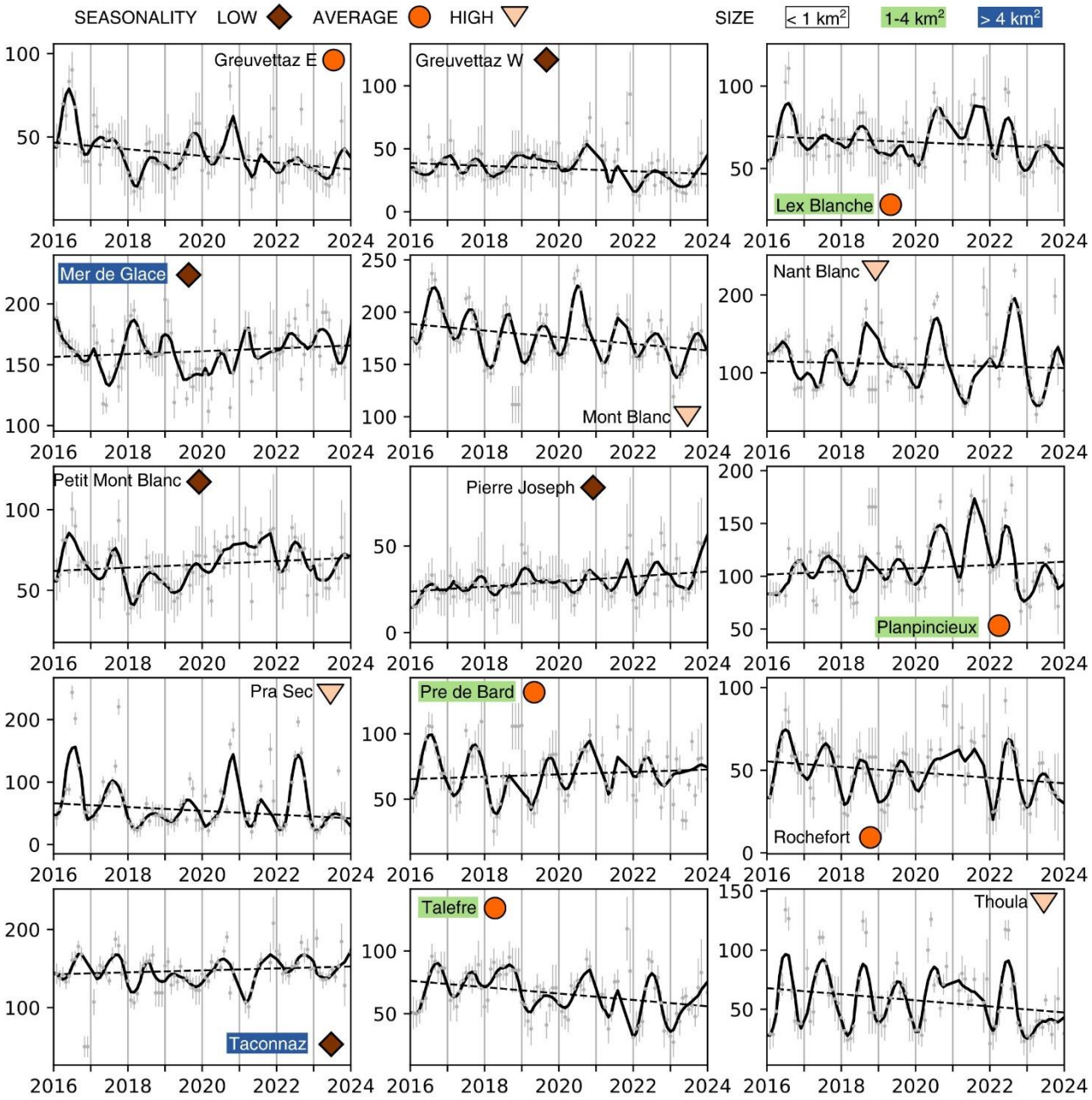

Fig. 6. Time series of monthly glacier surface velocities over the 2016-2024 period. Monthly raw data and corresponding uncertainty are depicted as grey dots and bars, while the solid black lines represent the LOWESS interpolation. The robust linear trends are represented in dashed black lines. The background colour of the glaciers' names denotes their size: white, green and blue are for small, medium and large glaciers, respectively. The velocity seasonality is indicated with markers: brown diamonds (low seasonality), orange circles (average seasonality) and pink rectangles (high seasonality).

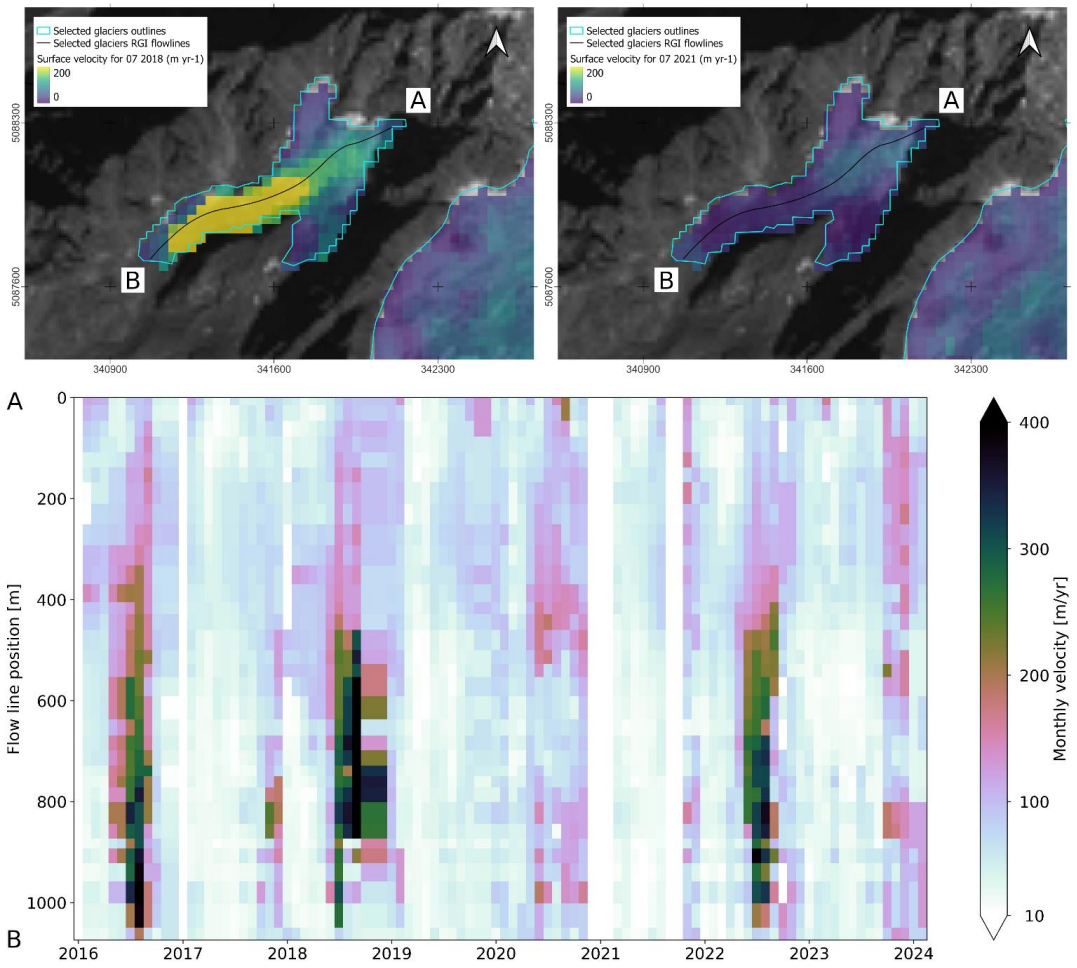

Fig. 7. Charpoua Glacier monthly surface velocity maps showing the spatial variation of the velocity patterns between July 2018 (upper left) and July 2021 (upper right). The lower panel shows the monthly velocity profiles along a longitudinal east-west AB profile (in black on the maps) over the study period. Sentinel-2 imagery base map (B08 band), courtesy of the Copernicus Open Access Hub (https://scihub.copernicus.eu, last access: 10 September 2023)

4.3 Interannual velocity variability and trend

The overall behaviour of the glacier velocity can be well represented by the PCA of the time series, weighted by the glacier area. Fig. 8 shows the 1st PC, which explained >50% of the variance. In general, this analysis reflects a common trend of many time series: a first period between 2016 and 2019 showing decreasing velocities, an anomaly of higher velocities between 2020 and 2022 followed by a new velocity decrease in 2023 (Fig. 6). According to historical observations at the Argentière and Miage glaciers, the velocity decrease from the early 2000s can be linked to continuous negative mass balances (Vincent and Moreau, 2016) of most Alpine glacier since the 2000s (Zemp et al., 2021). The results of our study agree with this negative trend in the first part of the considered period (i.e., 2016–2019). Still, we detected a rupture in the trend and a velocity rise from 2020 to 2022 occurring in many glaciers under study. An interesting remark about the geographical distribution of the trends is that the glaciers showing a clear velocity anomaly during 2020-2022 are located on the southeast side of the massif

ridgeline along the Italian and Swiss part of the Massif (e.g., A Neuve Central, Bionassay (IT), Brenva, Planpincieux and Lex Blanche glaciers). This might be linked to different dominant meteorological conditions distributions on the two sides of the massif. A specific analysis of seasonal meteorologic data in the different areas could give more insights into this hypothesis, even though whether stations are located far from the glacier accumulation areas and could not get a specific signal present in the higher altitude sectors.

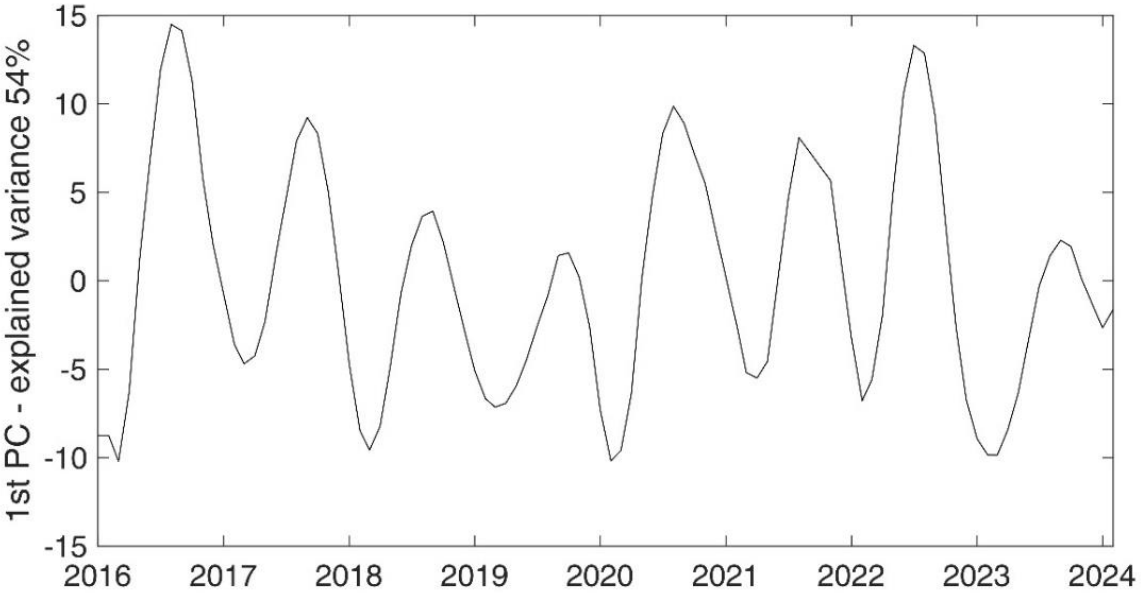

Fig. 8. 1st principal component (PC) of the LOWESS velocity values of all the time series of glacier monthly velocity.

The glacier velocities shown in Fig. 6 have different linear trends over the full period of the study (Fig. 9). In general, the linear trends of each glacier calculated using winter, summer months, or the whole year have similar behaviour (i.e., they are always negative or positive), with winter trends having higher absolute values than summer ones in case of positive acceleration and lower in case of negative acceleration (~30% difference on average). As expected, lower absolute linear trends (i.e., $\lesssim$1 m yr^{-2}) have *t*-statistics<2. Besides, although Brenva's trend is high (2.8 m yr^{-2}), its velocity is very large, thus lowering the *t*-statistics. Most trends lie in a relatively tight cluster which crosses the domain diagonally, except for Charpoua and Planpincieux which have dissimilar seasonal values. In the Charpoua case, this is probably related to the strong velocity fluctuations occurring only in some years in summer, while the Planpincieux positive summer trend is likely led by the anomaly 2020-2022, which is particularly strong in this glacier. Notably, the three glaciers with the highest linear trends (i.e., Freney, Bionassay (IT) and Aiguille de Tré-la-Tete) are all located in Val Veny, on the southern side of the massif. Bionassay (IT) and Freney have a very similar morphology (Tab. 1), they are both medium-size (1.3 km^2 and 1.02 km^2), relatively elongated (2.2 m^{-1} and 2.5 m^{-1}) glaciers, with slopes of ~25° and elevations between 2400 m a.s.l. and 3800 m a.s.l.. Differently, Aiguille de Tré-la-Tete is a small (0.3 km^2), much-elongated (4.34 m^{-1}) and low-altitude glacier (2408-3010 m a.s.l.). Aiguille de Tré-la-Tete and Bionassay (IT) are both tributaries of the Miage Glacier.

An accelerating trend (+5 m yr^{-2} between 2015-2021) has recently been shown for the Brenva Glacier by an analysis of remotely-sensed optical images (Rabatel et al., 2023b) while detecting decelerating trends on many other glaciers of the Massif. Our study showed Brenva Glacier an accelerating trend of +3 m yr^{-2} between 2016-2024, which is in good agreement considering the velocity decrease shown in 2022 and 2023 (a detailed comparison between this study and Rabatel et al. (2023b) is presented in Sec. S4). Besides, Rabatel et al. (2023b) observed a slight ice thickening (~1 m between 2000 and 2019) in an

upper sector of the Brenva Glacier, which agrees with the findings of Berthier et al. (2023) between 2012 and 2021, obtained with high-resolution satellite images. They proposed three hypotheses to explain the acceleration of the Brenva: a) a glacier thickening; b) a change in thermal regime; and c) a change in subglacial hydrology, possibly related to an increased ablation in the upper reaches of the glacier.

Even though the hypothesis of glacier thickening could explain the specific case of Brenva, the glacier surface elevation change across the Mont Blanc massif has been generally negative in the last years, as evidenced by the negative mass balance of the reference glaciers in the area (Zemp et al., 2021; Zemp et al., 2009) as well as massif scale studies (Berthier et al., 2023). Local anomalies of positive mass balance could explain an increase of velocity but the lack of measurements at higher altitudes does not allow us to confirm this behaviour. However, the meteorological conditions in recent years have remained approximately constant, which makes unlikely a general glacier thickening in the region (see S6 “Meteorological conditions”). Localized higher-than-usual accumulation rates due to increased avalanche activity and wind accumulation could also contribute to the ice thickening (thus yielding an acceleration) but cannot be investigated at this stage. It is worth noting that the three glaciers with high winter accelerating trends in Fig. 9 (Bionassay (IT), Aig Tré la Tete and Freney) are near to each other and located in a small part of the massif on its southeast side.

A change in the glaciers' thermal regime could explain accelerating trends, but it would explain long-term trends and not short-period variations such as the one highlighted in 2020-2022, as basal temperature measurements show a warming at the ice bedrock interface on a decadal to multi-decadal timescale on the Mont Blanc massif (Vincent et al., 2007).

A variation of the hydrology of groups of glaciers is a plausible hypothesis for the explanation of accelerating trends, but it would result in stronger trends in summer rather than in winter, as basal sliding is enhanced over deformation during summer. Such a combination of trends is not shown by most glaciers, as highlighted in Fig. 9. Only the trends of Planpincieux and Mer de Glace glaciers could relate well with this hypothesis, showing almost no trend in winter and an accelerating trend during the summer months.

The distribution of the acceleration trend over different areas of the massif and regarding different types of glaciers could suggest the existence of a meteo-climatic driver of the phenomenon, even though it is not evident, limiting the analysis to the period 2015-2023 (Section S6). In the end, a definitive answer cannot be formulated so far and further research is necessary to understand the processes involved in this trend.

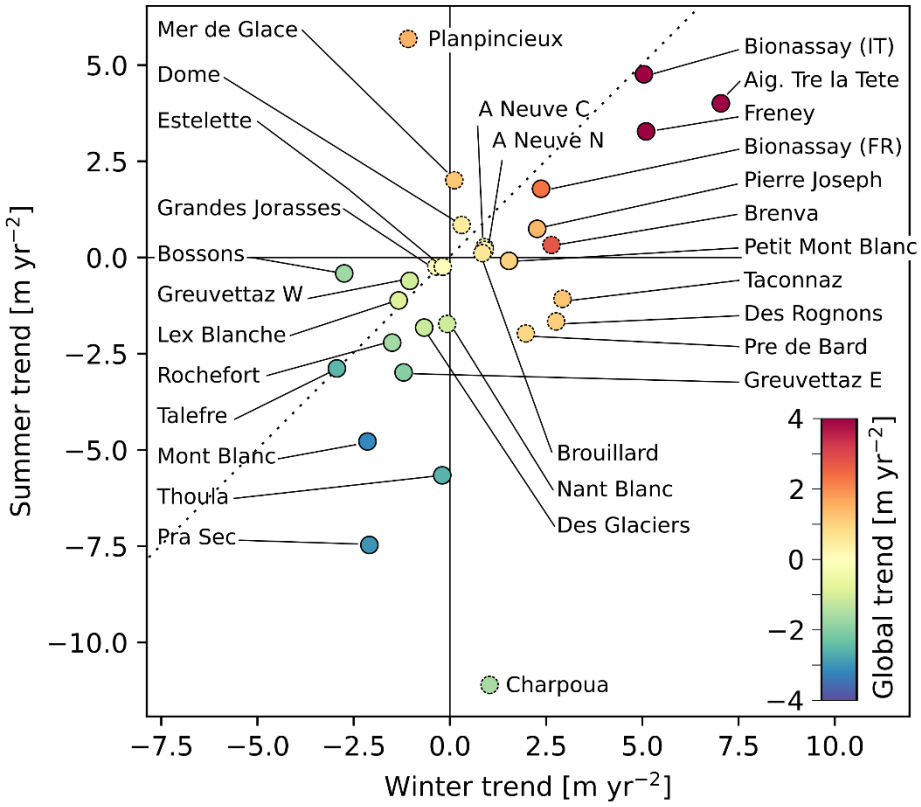

Fig 9. Linear trends of the glacier monthly velocity. The x- and y-axes refer to the trends calculated using winter (from November to April) and summer (from June to September) months, respectively. The colours indicate the global trend. The glaciers with linear trends with *t*-statictis<2 have markers with dashed edge lines.

4.4 Relationship between glacier size, velocity and seasonal behaviour

We examined the relationship between glacier size, seasonal velocity behaviour and monthly velocity distribution. To this end, we divided the glaciers into three classes for each feature. Concerning the size, we considered very small glaciers with an area of < 1 km^2, according to (Bahr and Radić, 2012), while medium and large glaciers have areas between 1 km^2 and 4 km^2, and >4 km^2, respectively. Concerning the velocity distribution, we observed that, besides Brenva and Bossons, which have much higher velocity compared to the rest of the glaciers, a group of sixteen glaciers have the 75th percentile of monthly velocity <100 m yr^{-1} (from Pierre Joseph to Charpoua in Fig. 5). Finally, twelve glaciers have their 25th and 75th percentiles between ~100 m yr^{-1} and ~200 m yr^{-1} (from Des Rognons to Freney in Fig. 5).

Concerning the seasonal velocity behaviour, we analysed the raw time series (Fig. 6) and the LOWESS smoothed time series normalised by their median value (Fig. S6). Glaciers such as Freney, Brouillard, and Bionassay (IT) show evident and regular seasonal behaviour and large winter/summer differences; in these cases, summer velocities (occurring between July and October) are 50% to 100% higher than winter ones (occurring between January and April). Another group of glaciers has smaller winter/summer differences or pronounced but irregular variability (e.g., Planpincieux, Pre de Bard, Talefre). A third group does not display evident or regular seasonal behaviour (e.g., Taconnaz, Mer de Glace, Pierre Joseph), with

winter/summer differences below 10%. Overall, the maximum velocity occurs in August-September, while the annual minimum is reached in March (Fig. 8).

The double-entry heatmaps are presented in Fig. 10, which show a tendency for the smaller glaciers to have more pronounced seasonality, while larger glaciers show a more homogeneous velocity throughout the year. Since the glacier area is strongly correlated with its thickness (Cuffey and Paterson, 2010), a possible cause of this phenomenon could be related to enhanced basal sliding during the accelerating period. In fact, a thicker glacier could be less prone to exhibit enhanced sliding because of the larger mass to be uplifted by basal positive water pressures. In contrast, shallower glaciers could more easily benefit from enhanced sliding by pressure build-up at the ice-bedrock interface by increasing inputs in the hydrological subglacial drainage network. Moreover, in winter, the base of thin glaciers could freeze, thus preventing the sliding and determining lower winter velocities, causing even larger summer-winter velocity differences.

On the other hand, as expected, larger (and thicker) glaciers tend to be faster than smaller ones.

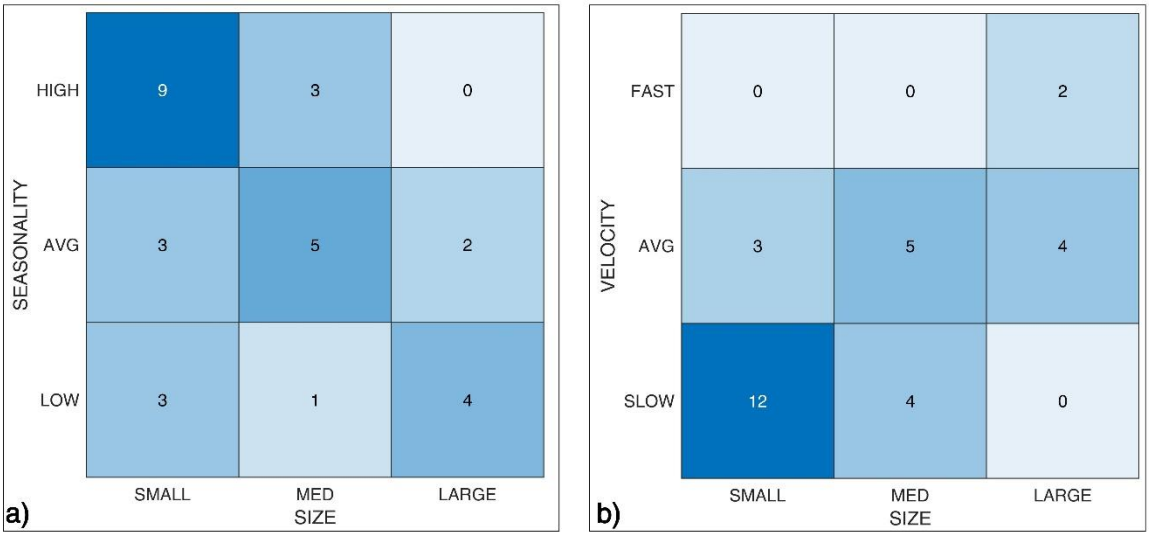

Fig. 10 Glacier classification according to their size (SMALL: <1 km^2; MED: 1-4 km^2; LARGE: >4 km^2) and a) seasonal velocity behaviour (qualitatively estimated) and b) median velocity (SLOW: <100 m yr^{-1}; AVG: 100-300 m yr^{-1}; FAST: >300 m yr^{-1}). The digits within the grid tiles indicate the number of glaciers belonging to each group.

4.5 Uncertainty analysis

To estimate the quality of our data, we performed two investigations. First, following the method proposed by (Millan et al., 2019), we calculated the median absolute deviation of the velocity obtained on stable terrain for each monthly data. In these areas, we applied an outlier spatial filter to the velocity maps according to Rabatel et al. (2023a). The median value of the monthly uncertainty was 10.9 m yr^{-1}. In their study, Millan et al. (2019) estimated the nominal precision according to the temporal baseline between the correlated images, which they found to be between 6–16 m yr^{-1} for baselines respectively of 40 and 20 days, which is the typical range of temporal gaps between images used in our study. Moreover, the value of 10.9 m yr^{-1} is in close agreement with the uncertainty found by Mouginot et al. (2023), which obtained a root mean squared error of 10.5 m yr^{-1} between glacier velocities measured over the Mer de Glace and Argéntiere glaciers using image correlation of Sentinel-2 images and GNSS in situ data (https://glacioclim.osug.fr/). A comparison with the data from Rabatel et al. (2023a) is proposed in the supplementary materials (Sec. S4, Fig. S3 and Tab. S1) for the glaciers of Brenva, Bionassay (FR), Bossons

and Brouillard over the timespan that overlaps the two studies (from February 2016 to December 2021), which evidences high agreement between the two studies.

Second, we considered the glacier velocity from Millan et al. (2019), who published mean annual velocity in the period 2017–2018 on a 50x50 m regular grid. They adopted normalised cross-correlation and chip size refinement (initial size of 16x16 px). They estimated an overall uncertainty of glacier surface velocity time series of ~12 m yr^{-1} over the Mont Blanc glaciers and, specifically at Brenva and Bosson glaciers, an uncertainty of 15–20 m yr^{-1}. We compared these data and ours along four glacier longitudinal central lines (i.e., in Bossons, Brenva, Freney and Taconnaz), obtaining good agreement (Fig. 11). The largest differences (>50 m yr^{-1}) were found in a specific sector of the Taconnaz Glacier (Fig. 11d), where the ice flux is highly channelized in a narrow passage. There, the data of Millan et al. (2019) show a large velocity decrease that seems unlikely considering the site's geometry. Our data show a similar but less pronounced velocity decrease. However, the velocity profiles are similar elsewhere. On average, the surface velocities we obtained are slightly higher, with a mean difference of 0.03 m yr^{-1} and root mean squared deviation (RMSD) of 24.0 m yr^{-1} (Table 2). The slightly higher RMSD compared to the expected uncertainty can be because the error over glacierized areas is probably larger than in ice-free zones because the surface texture is different and changes (e.g., snow precipitation, surface melt, glacier movement) occur more rapidly, therefore causing more decorrelation (Millan et al., 2019).

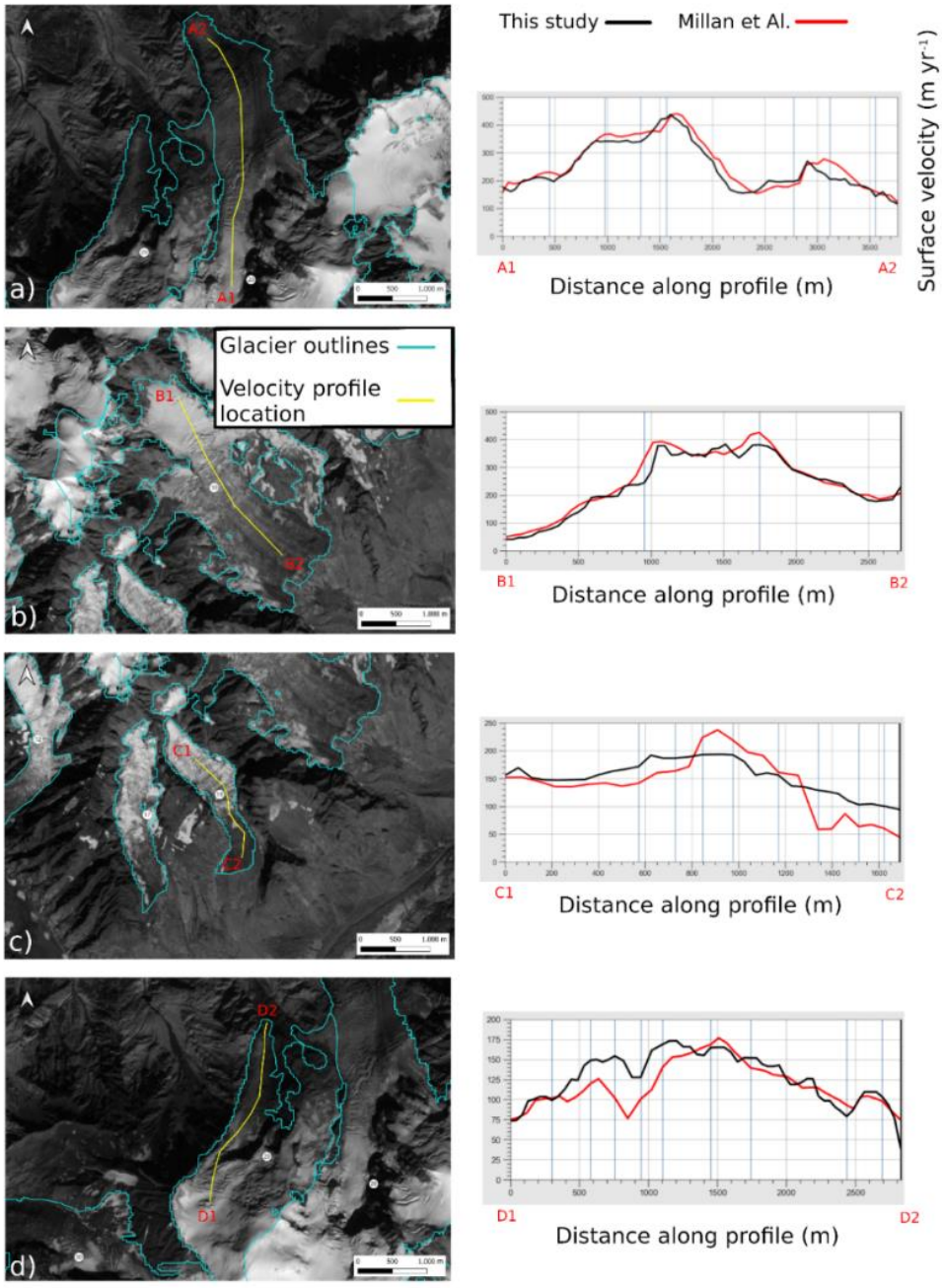

441

442 **Fig 11. Comparison of velocity profiles from Millan et al. (2022) (red) and from this study (black) at (a) Bossons**
443 **Glacier, (b) Brenva Glacier, (c) Freney Glacier and (d) Taconnaz Glacier. The velocity profiles are represented in**
444 **yellow in the maps on the left, and the velocity profiles start from the upper to the lower altitudes. Sentinel-2 image**
445 **base map (B08 band), courtesy of the Copernicus Open Access Hub (https://scihub.copernicus.eu, last access: 10**
446 **September 2023).**

Table 2. Mean difference and root mean squared deviation (RMSD) between this study and Millan et al. (2022) along velocity longitudinal profiles.

	Bossons	Brenva	Freney	Taconnaz	Mean all profiles
Mean difference [m yr^{-1}]	-13.1	-8.8	13.7	8.3	0.03
RMSD [m yr^{-1}]	22.3	25.2	29.6	19.0	24.0

4.6 Uses and limits of the proposed methodology

The methodology presented in this study allows the detection of monthly changes in glacier velocity, which can be precursors of ice avalanches (Pralong et al., 2005; Faillettaz et al., 2008; Giordan et al., 2020). For example, ice avalanches from the Pra Sec Glacier occurred in 2020 (Forestry Service of Aosta Valley). In our study, we observed high velocities in 2020, which could have led to the break-off. At the Charpoua Glacier, an ice avalanche of 45000 +/- 15000 m^3 occurred in 2018 (Lehmann, 2018 - https://news.unil.ch/display/1536777918113, accessed online 11 October 2023), when we measured velocities >200 m yr^{-1}, much higher than usual.

In this frame, measuring and knowing the typical velocity fluctuations of specific glaciers in stable conditions would be very relevant. This could allow an assessment and to what extent a suspect acceleration may be anomalous and potentially destabilising, bearing in mind that high-rate monitoring is essential to detect glacial instabilities since the expected sharp increase in velocity in the weeks before the failure (Pralong and Funk, 2006) could be hardly detectable from remote sensing (e.g., due to scarce visibility, image decorrelation, low resolution).

Limits of the methodology presented in this study should also be considered: glaciers moving at slow rates can be surveyed using temporal baselines of one year (Millan et al., 2019; Mouginot et al., 2023), but this implies losing the ability to catch short-term velocity fluctuations, like those observed at Charpoua and Pra Sec glaciers. Another known issue pertains to the lack of features of the glacier surface that make it impossible to track movements using optical imagery. Satellite optical imagery is limited and can be strongly influenced by the presence of clouds that could yield extensive periods without data acquisition, even though, in the present study, we had only four of 96 months with no data. Anomalies due to image decorrelation for the presence of shadows, snow or morphological surface modifications can occur and an expert-based visual check may be required to discriminate anomalous velocities.

6 Conclusions

We produced ice velocity maps and time series of thirty glaciers of the Mont Blanc massif during the period 2016–2024. The proposed results are different compared to the existing publicly available automatically processed velocity datasets that have a coarse resolution (i.e., >100 m) and cannot correctly detect the kinematics of most Alpine glaciers due to their small size. Therefore, specific processing and studies are needed to characterize the surface kinematics of Alpine glaciers. In our study, we used Sentinel-2 imagery due to its free availability, good ground resolution and high revisit time in the study area to obtain monthly surface velocity time series. In addition, we proposed a classification of different groups of glaciers based on their morpho-kinematic features. We also observed a significant acceleration trend in many of the studied glaciers in the last years (2020–2022), but the causes are still poorly understood.

From a methodological point of view, the proposed approach can be very useful to process and analyse available satellite images of other massifs in the Alps and other parts of the world. This approach could stimulate innovative research on high-resolution spatiotemporal variations of velocities on alpine glaciers and, especially, on understanding the variations in the motion of mountain glaciers. A large research question remains open and deals with understanding and measuring the drivers of change in the motion of alpine glaciers. This implies the complex acquisition of data related to the possible drivers of the variations, such as mass balances, water inputs and temporal variations in the subglacial hydrology of single glaciers. However, to delve further into these investigations, velocity databases at higher spatial and temporal resolutions, such as that presented in this study, are needed to build future research on the topic.

Acknowledgements

The authors would like to thank Jean Pierre Fosson, Raffaele Rocco, Valerio Segor, and Guido Giardini for their support and their will to stimulate cryospheric research activities in the Aosta Valley region and on the Italian side of Mont Blanc massif. We thank all the staff at Fondazione Montagna Sicura for supporting all the research activities of the research team. Dr Etienne Berthier supplied a processed 2018 Pleiades stereo DEM to retrieve altitudinal data presented in this paper. Dr. Antoine Rabatel supplied velocity data for the comparison with their 2023 dataset. We thank Dr. Christian Vincent for his advice on research activity and for supplying useful additional information, especially on the French glaciers of Mont Blanc.

Data availability

The following data are available for download on Zenodo http://dx.doi.org/10.5281/zenodo.11349445: i) monthly velocity maps, ii) updated outlines (from RGI7) of the analysed glaciers, iii) sampling areas of extraction of the velocity time series, iv) time series of monthly velocity. The data description and format are reported in Sec S9. Sentinel-2 imagery is available from the Copernicus Open Access Hub (https://scihub.copernicus.eu, Copernicus, 2022). The GIV toolbox is freely available online (https://github.com/MaxVWDV/glacier-image-velocimetry).

Competing interests. The authors declare that they have no conflict of interest.

Author contributions. Fabrizio Troilo: Conceptualization, writing – original draft preparation, investigation, methodology, data curation, formal analysis, visualization; Niccolò Dematteis: Writing – review & editing, data curation, methodology, formal analysis, validation, visualization; Francesco Zucca Writing – review & editing, methodology, supervision, validation; Martin Funk: Writing – review & editing, supervision; Daniele Giordan: Writing – review & editing, methodology, supervision, validation.

References

Ahn, Y. and Box, J. E.: Glacier velocities from time-lapse photos: technique development and first results from the Extreme Ice Survey (EIS) in Greenland, Journal of Glaciology, 56, 723-734, 2010.

Allstadt, K., Shean, D., Campbell, A., Fahnestock, M., and Malone, S.: Observations of seasonal and diurnal glacier velocities at Mount Rainier, Washington, using terrestrial radar interferometry, The Cryosphere, 9, 2219-2235, 2015.

Arendt, A., Bliss, A., Bolch, T., Cogley, J., Gardner, A., Hagen, J.-O., Hock, R., Huss, M., Kaser, G., and Kienholz, C.: Randolph Glacier inventory–A dataset of Global glacier outlines: Version 6.0: Technical report, Global land ice measurements from space, 2017.
Bahr, D. and Radić, V.: Significant contribution to total mass from very small glaciers, The Cryosphere, 6, 763-770, 2012.
Beniston, M., Farinotti, D., Stoffel, M., Andreassen, L. M., Coppola, E., Eckert, N., Fantini, A., Giacona, F., Hauck, C., and Huss, M.: The European mountain cryosphere: a review of its current state, trends, and future challenges, The Cryosphere, 12, 759-794, 2018.
Benn, D. I. and Evans, D. J.: Glaciers & glaciation, Routledge2014.
Beraud, L., Cusicanqui, D., Rabatel, A., Brun, F., Vincent, C., and Six, D.: Glacier-wide seasonal and annual geodetic mass balances from Pléiades stereo images: application to the Glacier d'Argentière, French Alps, Journal of Glaciology, 69, 525-537, 2023.
Berthier, E., Vadon, H., Baratoux, D., Arnaud, Y., Vincent, C., Feigl, K., Remy, F., and Legresy, B.: Surface motion of mountain glaciers derived from satellite optical imagery, Remote Sensing of Environment, 95, 14-28, 2005.
Berthier, E., Vincent, C., Magnússon, E., Gunnlaugsson, Á., Pitte, P., Le Meur, E., Masiokas, M., Ruiz, L., Pálsson, F., and Belart, J.: Glacier topography and elevation changes derived from Pléiades sub-meter stereo images, The Cryosphere, 8, 2275-2291, 2014.
Berthier, E., Vincent, C., and Six, D.: Exceptional thinning through the entire altitudinal range of Mont-Blanc glaciers during the 2021/22 mass balance year, Journal of Glaciology, 1–6, 2023.
Bindschadler, R.: The importance of pressurized subglacial water in separation and sliding at the glacier bed, Journal of Glaciology, 29, 3-19, 1983.
Cappellari, M., McDermid, R. M., Alatalo, K., Blitz, L., Bois, M., Bournaud, F., Bureau, M., Crocker, A. F., Davies, R. L., and Davis, T. A.: The ATLAS3D project–XX. Mass–size and mass–σ distributions of early-type galaxies: bulge fraction drives kinematics, mass-to-light ratio, molecular gas fraction and stellar initial mass function, Monthly Notices of the Royal Astronomical Society, 432, 1862-1893, 2013.
Cuffey, K. M. and Paterson, W. S. B.: The Physics of Glaciers, Academic Press2010.
Deilami, K. and Hashim, M.: Very high resolution optical satellites for DEM generation: a review, European Journal of Scientific Research, 49, 542-554, 2011.
Dematteis, N. and Giordan, D.: Comparison of digital image correlation methods and the impact of noise in geoscience applications, Remote Sensing, 13, 327, 2021.
Dematteis, N., Giordan, D., Troilo, F., Wrzesniak, A., and Godone, D.: Ten-Year Monitoring of the Grandes Jorasses Glaciers Kinematics. Limits, Potentialities, and Possible Applications of Different Monitoring Systems, Remote Sensing, 13, 3005, 2021.
Dematteis, N., Troilo, F., Scotti, R., Colombarolli, D., Giordan, D., and Maggi, V.: The use of terrestrial monoscopic time-lapse cameras for surveying glacier flow velocity, Cold Regions Science and Technology, 104185, 2024.
Einarsson, B., Magnússon, E., Roberts, M. J., Pálsson, F., Thorsteinsson, T., and Jóhannesson, T.: A spectrum of jökulhlaup dynamics revealed by GPS measurements of glacier surface motion, Annals of Glaciology, 57, 47-61, 2016.
Evans, A. N.: Glacier surface motion computation from digital image sequences, IEEE Transactions on Geoscience and Remote Sensing, 38, 1064-1072, 2000.
Fahnestock, M., Scambos, T., Moon, T., Gardner, A., Haran, T., and Klinger, M.: Rapid large-area mapping of ice flow using Landsat 8, Remote Sensing of Environment, 185, 84-94, 2016.
Faillettaz, J., Pralong, A., Funk, M., and Deichmann, N.: Evidence of log-periodic oscillations and increasing icequake activity during the breaking-off of large ice masses, Journal of Glaciology, 54, 725-737, 2008.
Fyffe, C. L.: The hydrology of debris-covered glaciers, University of Dundee, 2012.
Giordan, D., Dematteis, N., Allasia, P., and Motta, E.: Classification and kinematics of the Planpincieux Glacier break-offs using photographic time-lapse analysis, Journal of Glaciology, 66, 188-202, 2020.
Glen, J.: Experiments on the deformation of ice, Journal of Glaciology, 2, 111-114, 1952.
Gottardi, F., Obled, C., Gailhard, J., and Paquet, E.: Statistical reanalysis of precipitation fields based on ground network data and weather patterns: Application over French mountains, Journal of hydrology, 432, 154-167, 2012.
Heid, T. and Kääb, A.: Evaluation of existing image matching methods for deriving glacier surface displacements globally from optical satellite imagery, Remote Sensing of Environment, 118, 339-355, 2012.

Huber, P. J.: Robust estimation of a location parameter, in: Breakthroughs in statistics: Methodology and distribution, Springer, 492-518, 1992.
Humbert, A., Greve, R., and Hutter, K.: Parameter sensitivity studies for the ice flow of the Ross Ice Shelf, Antarctica, Journal of Geophysical Research: Earth Surface, 110, 2005.
Jiskoot, H.: Dynamics of Glaciers, physical Research, 92, 9083-9100, 2011.
Jolliffe, I. T. and Cadima, J.: Principal component analysis: a review and recent developments, Philosophical transactions of the royal society A: Mathematical, Physical and Engineering Sciences, 374, 20150202, 2016.
Kääb, A., Winsvold, S., Altena, B., Nuth, C., Nagler, T., and Wuite, J.: Glacier Remote Sensing Using Sentinel-2. Part I: Radiometric and Geometric Performance, and Application to Ice Velocity, Remote Sensing, 8, 2016.
Kääb, A., Jacquemart, M., Gilbert, A., Leinss, S., Girod, L., Huggel, C., Falaschi, D., Ugalde, F., Petrakov, D., and Chernomorets, S.: Sudden large-volume detachments of low-angle mountain glaciers–more frequent than thought?, The Cryosphere, 15, 1751-1785, 2021.
Kamb, B.: Glacier surge mechanism based on linked cavity configuration of the basal water conduit system, Journal of Geophysical Research: Solid Earth, 92, 9083-9100, 1987.
Luzi, G., Pieraccini, M., Mecatti, D., Noferini, L., Macaluso, G., Tamburini, A., and Atzeni, C.: Monitoring of an alpine glacier by means of ground-based SAR interferometry, IEEE Geoscience and Remote Sensing Letters, 4, 495-499, 2007.
Marsy, G., Vernier, F., Trouvé, E., Bodin, X., Castaings, W., Walpersdorf, A., Malet, E., and Girard, B.: Temporal Consolidation Strategy for Ground-Based Image Displacement Time Series: Application to Glacier Monitoring, IEEE Journal of Selected Topics in Applied Earth Observations and Remote Sensing, 14, 10069-10078, 2021.
Millan, R., Mouginot, J., Rabatel, A., and Morlighem, M.: Ice velocity and thickness of the world's glaciers, Nature Geoscience, 15, 124-129, 2022.
Millan, R., Mouginot, J., Rabatel, A., Jeong, S., Cusicanqui, D., Derkacheva, A., and Chekki, M.: Mapping surface flow velocity of glaciers at regional scale using a multiple sensors approach, Remote Sensing, 11, 2498, 2019.
Mondardini, L., Perret, P., Frasca, M., Gottardelli, S., and Troilo, F.: Local variability of small Alpine glaciers: Thoula Glacier geodetic mass balance reconstruction (1991-2020) and analysis of volumetric variations, Geografia Fisica e Dinamica Quaternaria, 44, 29-38, 2021.
Mouginot, J., Rabatel, A., Ducasse, E., and Millan, R.: Optimization of Cross Correlation Algorithm for Annual Mapping of Alpine Glacier Flow Velocities; Application to Sentinel-2, IEEE Transactions on Geoscience and Remote Sensing, 61, 1-12, 2023.
Nesje, A.: Topographical effects on the equilibrium-line altitude on glaciers, GeoJournal, 27, 383-391, 1992.
Nye, J. F.: The mechanics of glacier flow, Journal of Glaciology, 2, 82-93, 1952.
Paul, F., Winsvold, S. H., Kääb, A., Nagler, T., and Schwaizer, G.: Glacier remote sensing using Sentinel-2. Part II: Mapping glacier extents and surface facies, and comparison to Landsat 8, Remote Sensing, 8, 575, 2016.
Paul, F., Piermattei, L., Treichler, D., Gilbert, L., Girod, L., Kääb, A., Libert, L., Nagler, T., Strozzi, T., and Wuite, J.: Three different glacier surges at a spot: what satellites observe and what not, The Cryosphere, 16, 2505-2526, 2022.
Paul, F., Rastner, P., Azzoni, R., Diolaiuti, G., Fugazza, D., Le Bris, R., Nemec, J., Rabatel, A., Ramusovic, M., and Schwaizer, G.: Glacier shrinkage in the Alps continues unabated as revealed by a new glacier inventory from Sentinel-2, Earth Syst. Sci. Data, 12, 1805–1821, 2020.
Pfeffer, W. T., Arendt, A. A., Bliss, A., Bolch, T., Cogley, J. G., Gardner, A. S., Hagen, J.-O., Hock, R., Kaser, G., and Kienholz, C.: The Randolph Glacier Inventory: a globally complete inventory of glaciers, Journal of glaciology, 60, 537-552, 2014.
Pralong, A. and Funk, M.: On the instability of avalanching glaciers, Journal of Glaciology, 52, 31-48, 2006.
Pralong, A., Birrer, C., Stahel, W. A., and Funk, M.: On the predictability of ice avalanches, Nonlinear Processes in Geophysics, 12, 849-861, 2005.
Rabatel, A., Ducasse, E., Millan, R., and Mouginot, J.: Satellite-Derived Annual Glacier Surface Flow Velocity Products for the European Alps, 2015–2021, Data, 8, 66, 2023a.
Rabatel, A., Ducasse, E., Ramseyer, V., and Millan, R.: State and Fate of Glaciers in the Val Veny (Mont-Blanc Range, Italy): Contribution of Optical Satellite Products, Journal of Alpine Research| Revue de géographie alpine, 2023b.
Rankl, M., Kienholz, C., and Braun, M.: Glacier changes in the Karakoram region mapped by multimission satellite imagery, The Cryosphere, 8, 977-989, 2014.

RGI Consortium: Randolph Glacier Inventory - A Dataset of Global Glacier Outlines, Version 7 [Data Set], Boulder, Colorado USA. National Snow and Ice Data Center. https://doi.org/10.5067/F6JMOVY5NAVZ. (2023) Date Accessed 03-26-2024.
Samsonov, S., Tiampo, K., and Cassotto, R.: SAR-derived flow velocity and its link to glacier surface elevation change and mass balance, Remote Sensing of Environment, 258, 112343, 2021.
Scambos, T. A., Dutkiewicz, M. J., Wilson, J. C., and Bindschadler, R. A.: Application of image cross-correlation to the measurement of glacier velocity using satellite image data, Remote sensing of environment, 42, 177-186, 1992.
Schwalbe, E. and Maas, H.-G.: The determination of high-resolution spatio-temporal glacier motion fields from time-lapse sequences, Earth Surface Dynamics, 5, 861-879, 2017.
Somigliana, C.:Meccanica e termodinamica dei ghiacciai, Seminario Mat. e. Fis. di Milano 12, 72–84, 1938.
Span, N. and Kuhn, M.: Simulating annual glacier flow with a linear reservoir model, Journal of Geophysical Research: Atmospheres, 108, 2003.
Stocker-Waldhuber, M., Fischer, A., Helfricht, K., and Kuhn, M.: Long-term records of glacier surface velocities in the Ötztal Alps (Austria), Earth system science data, 11, 705-715, 2019.
Van Wyk De Vries, M. and Wickert, A. D.: Glacier Image Velocimetry: an open-source toolbox for easy and rapid calculation of high-resolution glacier velocity fields, The Cryosphere, 15, 2115-2132, 10.5194/tc-15-2115-2021, 2021.
Vincent, C., Soruco, A., Six, D., and Le Meur, E.: Glacier thickening and decay analysis from 50 years of glaciological observations performed on Glacier d'Argentière, Mont Blanc area, France, Ann. Glaciol., 50, 73–79, 2009.
Vincent, C. and Moreau, L.: Sliding velocity fluctuations and subglacial hydrology over the last two decades on Argentière glacier, Mont Blanc area, Journal of Glaciology, 62, 805-815, 2016.
Vincent, C., Le Meur, E., Six, D., Possenti, P., Lefebvre, E., and Funk, M.: Climate warming revealed by englacial temperatures at Col du Dôme (4250 m, Mont Blanc area), Geophysical Research Letters, 34, 2007.
Willis, I. C.: Intra-annual variations in glacier motion: a review, Progress in Physical Geography, 19, 61-106, 1995.
Zekollari, H., Huss, M., and Farinotti, D.: Modelling the future evolution of glaciers in the European Alps under the EURO-CORDEX RCM ensemble, The Cryosphere, 13, 1125-1146, 2019.
Zemp, M., Hoelzle, M., and Haeberli, W.: Six decades of glacier mass-balance observations: a review of the worldwide monitoring network, Annals of Glaciology, 50, 101-111, 2009.
Zemp, M., Nussbaumer, S. U., Gärtner-Roer, I., Bannwart, J., Paul, F., and Hoelzle, M.: Global Glacier Change Bulletin Nr. 4 (2018-2019), WGMS, 4, 2021.
Zemp, M., Huss, M., Eckert, N., Thibert, E., Paul, F., Nussbaumer, S. U., and Gärtner-Roer, I.: Brief communication: Ad hoc estimation of glacier contributions to sea-level rise from the latest glaciological observations, The Cryosphere, 14, 1043-1050, 2020.